

Irradiation of polymer foil using single MeV-energy heavy ions

Nora Reinić

Physics Department, Faculty of Science, Bijenička 32, Zagreb

Supervisor: Georgios Provatas

Ruder Bošković Institute, Bijenička 54, Zagreb

(Dated: January 2021.)

Abstract

When irradiating a thin polymer foil with single heavy ions of MeV-energies, the cylindrical regions of aggregated defects, called latent tracks, are formed along the ion's trajectory. Since these regions of damage are quite small, around few nm in diameter, they can only be visible with transmission electron microscope. Nevertheless, they show the increased chemical activity and, when immersed in a suitable chemical solution, these damaged zones can get preferentially dissolved. Such a procedure is called chemical etching and it enlarges the track dimensions, thus creating the pores visible even with the optical microscope. In this experiment, carbon ions of 20 MeV energy are accelerated and directed through the 6 μm thin polycarbonate foil. Using a scanning system, carbon ions are focused one by one in a 32 x 32 rectangular pattern with $\sim 10 \mu\text{m}$ spacing between them. After the irradiation, the track-etching is performed in controlled conditions using the KOH solution as an etching medium. In the end, the foil sample was thoroughly examined with the optical microscope and the pores created by ions were observed.

I. INTRODUCTION

I.1. Formation of the latent tracks

It is well known that the passing of a charged ion through dielectric material gives rise to an abundance of various effects in the material's structure. Although the time the ion spends in the vicinity of the atoms in the solid is quite short ($\sim 10^{-17}$ s for an ion with the velocity of $\approx 10\%$ of the speed of light), this primary interaction causes the electron collision cascade. The electron collision cascade spreads along the trajectory for the next $\sim 10^{-14}$ s, leaving an extremely unstable structure of mutually repulsive positively charged nuclei. Because of the Coulomb repulsion, such a structure results in a process called "Coulomb explosion", triggering the rapid ejections of the leftover positive ions onto the interstitial positions. Around $\sim 10^{-12}$ s later, the cloud of point defects is left behind. As a consequence of the previous interactions, a very hot cylindrical region is created around the ion's trajectory. During the cooling, the defects tend to aggregate, and a so-called track core is formed in a diameter of about 10 nm. It is worth noting that the radius of a track core, created by atomic collisions, is several orders of magnitude smaller in comparison to the radial range of electronic collision cascade.

Organic polymer materials are much more sensitive to the irradiation damage in comparison to the inorganic ones. This is due to the fact that, in polymers, electron collisions can cause breaking or linking of the long chain molecules, which results in the creation of many chemically reactive products. Therefore, the severely damaged region extends not only to the track core, but also to the surrounding halo, as schematically depicted on Figure 1.

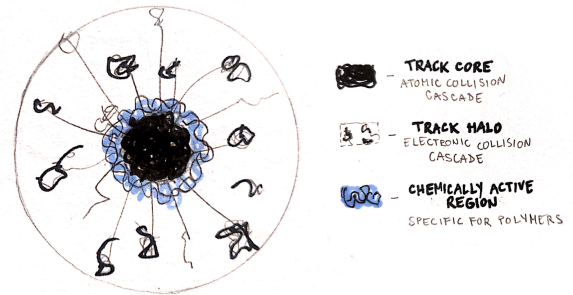


Figure 1: Schematic representation of radial cut through the latent track in polymer. The track core has a diameter of around 10 nm and the surrounding track halo has a diameter of around 1000 nm. Specifically in polymer materials, a chemically active region is formed around the track core and its diameter extends to around 100 nm.

In case of heavy ions of energy in MeV or GeV range, such created damaged zones can be quasi-stable or stable and, therefore, the single ion trails can be permanently recorded in the dielectric solids, opening a door for various applications. These permanent trails are called latent tracks and many theories have been developed trying to quantify the conditions and requirements for their occurrence. The important quantity known to be directly related to the remaining damage and the formation of latent tracks is the stopping power of an ion. This term refers to the ion energy loss per unit length of the path and, the larger it is, the more damage is created in a material. Therefore, for a latent track to be registered, the stopping power must exceed a threshold value specific for each material. Since, in the experiment, the ion energy is a property we can control, it is crucial to analyse how it influences the stopping power. Although a lot of theoretical research is involved in analytical describing of this dependence, for the purposes of this paper it is more useful to describe the occurring phenomena qualitatively.

I.2. Stopping power

There are two distinctive stopping mechanisms. For low energy ions, the main contribution to the energy loss comes from the interactions of the ion and the target material nuclei. In this regime of nuclear stopping, collisions are causing the abrupt changes in ion's energy and direction, creating a secondary atomic cascade for which the created damage can be registered not only in dielectric materials, but also in semiconductors and conductors. Nevertheless, these collisions are drastically decreasing the ion's velocity so it reaches its final stopping point in a very short time. For that reason, low energy ions are not convenient for creating the latent tracks.

For high energy ions, the energy loss is dominated by electron stopping, corresponding to the interactions of the ion and the target electrons. Contrary to the nuclear collisions, the electron collisions do not significantly change the ion's direction and, therefore, electronic stopping slows down the ion in a rather smooth way.

Figure 2 shows how the both electronic and nuclear stopping power depend on specific energy of a heavy ion. As can be seen, the nuclear stopping power indeed dominates for low specific energies and electronic stopping power dominates for higher specific energies. On its way through the solid, the heavy ion of a very high initial specific energy would first be completely stripped out of its electrons. At that instance, its energy loss is too small to produce the damage in a form of a latent track. As its velocity decreases, the ion starts capturing the electrons back and, consequently, the electron stopping power increases. At some point, usually around 1-10 MeV/nucleon, the stopping power reaches its maximum value. Slowing down even more, the energy loss reduces and soon again falls below the latent track formation threshold value¹.

Hence, if one wants to imprint a latent track in a solid, he must carefully examine the stopping power curve and choose the appropriate projectile energy. Since the calculation of the required energy (and all the other parameters) for the experiment would be quite complicated to do by hand, software programs which simulate the ion-target interactions based on the initial properties are developed. One of them, SRIM, is used for this experiment and is further described in Experimental method section.

I.3. Chemical etching

The latent tracks are, in fact, quite small (around several nm) and they can only be visible with transmission electron microscopes, what might complicate their examination and limit their applications. Therefore, for practical purposes, it is convenient to apply a procedure which results in their enlargement. Chemical etching is one of such procedures and it exploits the fact that damaged regions are more sensitive

to the chemicals compared to the bulk material. Immersing the irradiated material in a suitable solution triggers the intensive chemical reactions along the latent tracks and, eventually, these damaged zones get dissolved. Therefore, chemical etching serves as an amplifier for existing inhomogeneities and, if performed in suitable conditions, can enlarge the track intersection up to the order of magnitude of μm .

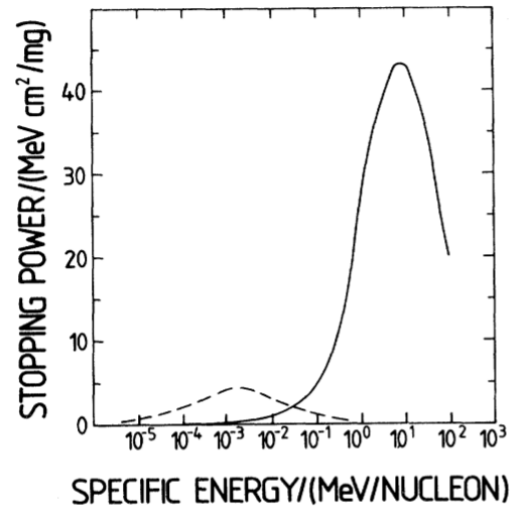


Figure 2: Specific stopping power of a heavy ion in solid. The full line represents the electronic stopping power and the dashed line represents the nuclear stopping power².

The property which characterizes the speed of etching in a material is called the etch rate. In order to remove only the cylindrical regions around the track core, the ratio of the radial track etch rate and the bulk etch rate should be sufficiently high³. As already mentioned, the damaged regions with high density of defects show the increased chemical activity, which results in a higher radial etch rate compared to the much more stable bulk material. Since in polymers the disordered region extends radially further compared to the inorganic dielectrics, they represent the attractive candidates for exploring this technique.

I.4. Track imprinting applications

In this experiment we used the described nuclear track imprinting procedure with the aim of producing a regular pattern of pores on a thin polycarbonate foil. Foils with etched nuclear tracks have a broad range of applications in numerous scientific and industrial fields. Their big advantage is that created pores are highly stable and their dimensions can be adjusted by controlling the etching conditions. By irradiating a foil with only one ion, very precise bio-sensors, such as single DNA molecule sensors⁴, can be produced. Moreover, the pores can be made to create very selective filters, or to mimic ion channels in biological cell membranes⁵. Their application extends to the nanotechnologies where the etched tracks serve as templates and can be filled with an appropriate material to make

nanostructures such as nanowires. Finally, with modern ion beam facilities, arranging the tracks in a predetermined regular pattern is possible and can be useful in electronics and many more fields where the structures are required to be positioned with a very high precision⁶.

II. EXPERIMENTAL METHOD

The experiment was carried out at the Laboratory for ion beam interactions at the Ruđer Bošković Institute (RBI) in Zagreb, Croatia. The facility consists of two tandem accelerators connected to multiple experimental beam lines with different purposes. For this experiment, the ions were generated in the ion source and accelerated with 6.0 MV EN Tandem Van de Graaf accelerator (Figure 3). Using a magnetic field, the beam was further directed towards the ion microprobe beam line.



Figure 3: 6.0 MV EN Tandem Van de Graaf accelerator at RBI research facility.

II.1. Ion microprobe

Ion microprobe is a device which focuses the beam to the target with a very high precision and scans the millimeter-dimension surface of the sample. The beam spot size depends on ion species being focused, their energy and current. It can be used for a wide range of material analysis techniques, for example particle induced X-ray spectroscopy (PIXE), Rutherford backscattering (RBS) and scanning transmission ion microscopy (STIM). The device can be adjusted to high and low current operation modes. In the high current mode, the currents are between 1 and 1000 pA and the beam spot size can be as low as 1 mm. For the low current mode, the current is <1 fA and its beam spot size can reach the precision up to 250 nm. This mode can be used for irradiating the samples with single ions.

The schematic setup of the ion microprobe is shown on Figure 4. On its way to the target, the ion current is first arbitrarily reduced with three pairs of slits. Then it passes through the beam scanner, composed of two dipole magnets controlled by

the SPECTRUM software, and is further focused by the system of magnetic quadrupoles. The target chamber is equipped with several detectors and a camera with view field of 2.5 mm so that sample can be viewed on a computer monitor⁷. In order to avoid the external interference, the interior of the beam line and the target chamber must be under extreme vacuum, which is achieved using a cascade of a mechanical and turbomolecular vacuum pump.

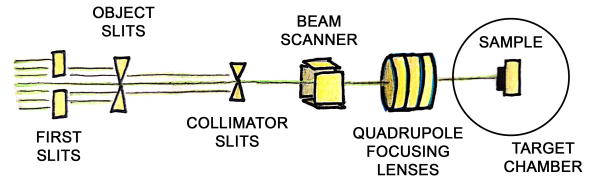


Figure 4: Schematic sketch of the ion microprobe setup.

In this experiment, we wanted to irradiate a 6 μm thin polycarbonate foil with single ions in order to create a rectangular pattern of latent track pores. Such a regular pattern is created with the beam scanner, and we can adjust the order of scanning (Figure 5) and the distance between the spots. The dimensions of the irradiated area for certain scanning pattern can be calculated by irradiating an additional reference sample of the known grid dimensions. The device must operate in a low current mode, letting the ions pass to the target one by one. In the experiment, the incoming ions hit the target perpendicular to the surface and pass through it. Each transmitted ion then triggers the Si particle detector and the beam is switched to the next position.

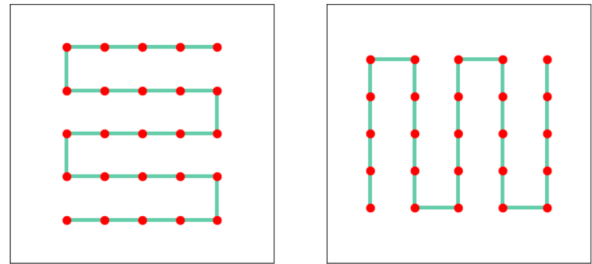


Figure 5: Different orders of beam movement over the sample during scanning.

II.2. SRIM software

For irradiation, we used 20 MeV carbon ions. To be sure that these ions would completely pass through the foil instead of stopping inside of it, the stopping ranges of different ions in a polycarbonate target were computed with the SRIM program before performing the experiment. SRIM is a collection of software packages which calculates different features of the transport of ions in matter. Based on the input ion species, energy and target composition, it can calculate the

stopping power and range of ions taking into account the important physical interactions. Of course, the exact computing of all interactions on the ion's path through the target would be extremely inefficient, so the program uses statistical approaches with theoretical and experimental data embedded in the algorithms.⁸

Figure 6 shows the stopping ranges of several ion species in a polycarbonate target for different projectile energies. In general, ions with larger mass have a shorter stopping range. As can be seen from the plot, 20 MeV carbon ions have a range of $\approx 25 \mu\text{m}$, which is more than enough to pass through a $6 \mu\text{m}$ foil. The computed stopping power curves for different ions are plotted on Figure 7. We can see that heavier ions have a larger stopping power. Therefore, very light ions cannot be used to produce the latent tracks.

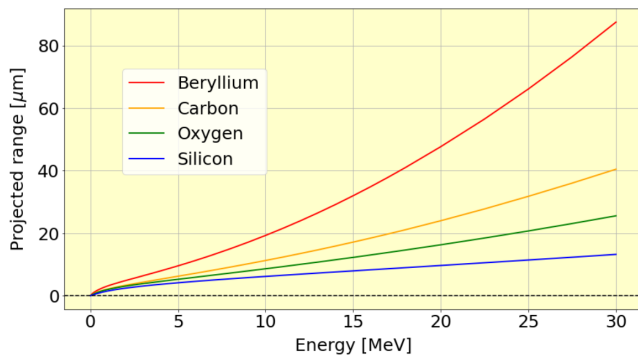


Figure 6: Projected ranges computed with SRIM for different ion species.

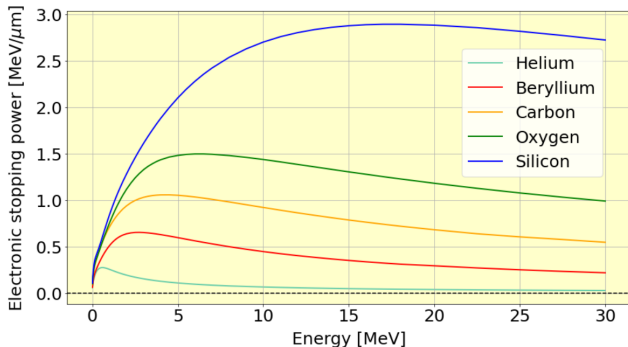


Figure 7: Electronic stopping power curves computed with SRIM for different ion species.

II.3. Chemical etching recipe

After irradiating the foil, with the aim to enlarge the latent tracks to dimensions visible with the optical microscope, chemical etching was performed by the following recipe. 200 mL of KOH solution with concentration of 3 mol/L was prepared in a beaker. The solution was heated to the temperature of $50 \text{ }^\circ\text{C}$ and the foil was immersed in it for 40 minutes. Since during the entire etching process the sample should be

completely surrounded by the solution, we fixated it with the tweezers in order to prevent touching the edges of a beaker.

After the etching, the sample was left to dry for several days. In the end, created pores were examined with the optical microscope.

III. RESULTS AND DISCUSSION

A $6 \mu\text{m}$ thin polycarbonate foil was scanned with 20 MeV carbon ions in order to create a rectangular pattern of 32×32 ion spots on six different areas of the foil's surface. The diameter of the entire foil sample was 1.5 cm and each of the irradiated areas covered a surface of less than $1 \times 1 \text{ mm}$. The scanning of different irradiated areas differed in the following parameters: scanned area size (dimension of the longer side of the rectangle: $(213 \pm 5) \mu\text{m}$ or $(426 \pm 5) \mu\text{m}$), number of ions per trigger (1 or 2 ions/trigger) and order of scanning (Figure 5).

Few days later, chemical etching was performed following the above described procedure. After drying, it was examined with the optical microscope. The process of searching for the pores was not a straightforward task because, although not visible with the eye, this foil had plenty of other minor damages over its surface. Also, the foil itself is quite thin so it was not possible to perfectly stretch it over the glass and avoid the folds. Another circumstance which made recognizing the pores difficult was that the entire foil area is big in comparison to the microscope field of view. The sample was mostly observed at $10\times$ magnification, which corresponds to the field of view with $\approx 50 \mu\text{m}$ diameter.

Eventually, the pores were found and the pictures are shown on Figure 8, together with the scale. The distance between the two ticks on the scale is $10 \mu\text{m}$. From the obtained pictures it can be seen that the pores really are arranged in a regular pattern, although they do not seem to be of equal sizes. The latter might be due to the distortion of the image caused by the folds on a foil. The pattern dimensions correspond to the expected ones. Furthermore, it is possible to distinguish the pores corresponding to one ion per spot (Figure 8a) from the ones corresponding to two ions per spot (Figure 8b). In order to examine their shape more closely, the additional pictures were taken with magnification of $40\times$ and $60\times$, and are shown on Figure 9.

The experiment results are satisfactory, but the improvements could be made. Since, as can be seen in the pictures, even the very small damages of the foil surface are clearly visible under the microscope, to obtain better results and clearer pictures one should be more careful in handling the foil, trying to minimize the contact with the surrounding surfaces. Further, more care should be devoted to fixating and stretching the foil over a sample holder because each of the small folds significantly alters the image under the microscope, thus disabling the accurate determination of dimensions of the structures.

Unfortunately, because of the above mentioned difficulties, especially the limited field of view, it could not be recognized which of the observed pores correspond to which of the six scanned regions. Therefore, it can be concluded that in fu-

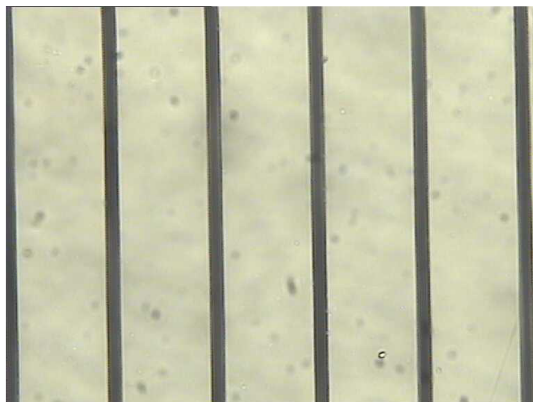
ture experiments of this kind, each irradiated area should be marked during the scanning. This marker could be, for example, a big, easily noticeable irradiation damage focused very near the each region scanned.



a)

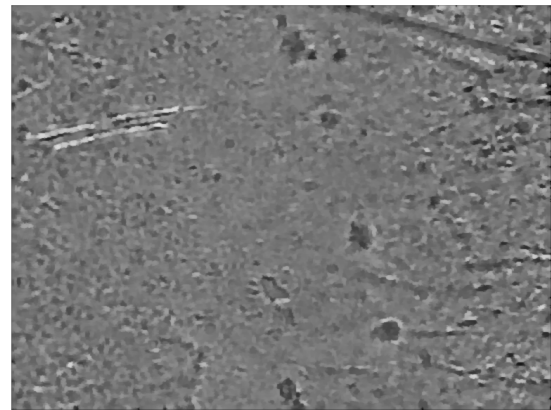


b)

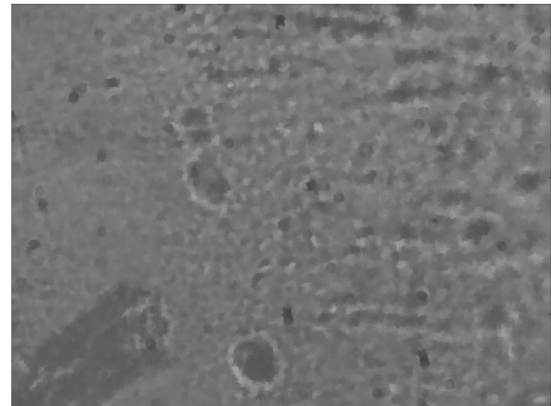


c)

Figure 8: Figures a) and b) show the etched pores under the optical microscope with magnification of 10x. Image c) shows the scale with 10 μm distance between the ticks.



a)



b)

Figure 9: Etched pores under the optical microscope with magnification of a) 40x and b) 60x.

IV. CONCLUSION

In this experiment, we irradiated a 6 μm thin polycarbonate foil with single 20 MeV carbon ions to create the permanent damage in a form of latent tracks. The experiment was carried out at the RBI research facility where the ions were accelerated with the EN Tandem accelerator and focused with the ion microprobe. Using a scanning system, the ions were focused to create a rectangular pattern of latent track pores on a foil surface. 6 different spots on a foil were irradiated using different scanning parameters. Furthermore, by performing chemical etching, the tracks were successfully enlarged to a size visible with the optical microscope. While searching for the track pores with the optical microscope, several difficulties were encountered. These were due to the other minor damages and folds on the sample's surface, as well as the microscope's limited field of view. In the end, the pores were found, visibly arranged in an approximately regular pattern. What couldn't be recognized is which of the observed pores correspond to which of the six scanned regions. Hence, it is recommended that

in future track imprinting experiments, each irradiated area is marked during the scanning with a bigger, easily noticeable irradiation damage focused next to it.

V. ACKNOWLEDGMENTS

I would like to thank the laboratory leader Milko Jakšić for the opportunity to work at the RBI experimental facility, my supervisor Georgios Provatas for all the help in carrying out the experiment and operating the experimental setup, Kristina Tomić Luketić for help with preparing and performing the etching and all the others at RBI who assisted me during this work.

-
- ¹ B. E. Fischer, R. Spohr (1983), *Production and use of nuclear tracks: imprinting structure on solids*, Rev. Mod. Phys. 55, 907-948.
- ² H. Geissel (1982), *Untersuchungen zur Abbremsung von Schwerionen in Materie im Energiebereich von (0.5–10) MeV/u*, Gesellschaft für Schwerionenforschung Report 82-12.
- ³ A.M. Bhagwat (1993), *Solid State Nuclear Track Detection: Theory and Applications*, ISRP-K-TD-2.
- ⁴ A. Mara, Z. Siwy, C. Trautmann, J. Wan, F.Kamme (2004) *An Asymmetric Polymer Nanopore for Single Molecule Detection*, Nano Letters, 4, 3, 497–501.
- ⁵ N. Sertova, E. Balanzat, M. Toulemonde, C. Trautmann (2009), *Investigation of initial stage of chemical etching of ion tracks in polycarbonate*, Nuclear Inst. and Methods in Physics Research, B / 267(6), 1039-1044.
- ⁶ A. Waheed, D. Forsyth, A. Watts, A.F. Saad, G.R. Mitchell, M. Farmer, P.J.F. Harris (2009), *The track nanotechnology*, Radiation Measurements 44(9-10), 1109-1113.
- ⁷ Ruder Bošković Institute, *Laboratory for ion beam interactions*. Retrieved from <https://www.irb.hr/eng/Divisions/Division-of-Experimental-Physics/Laboratory-for-ion-beam-interactions>
- ⁸ J. Ziegler, *SRIM & TRIM*. Retrieved from <http://www.srim.org/>